Colloids and Surfaces B: Biointerfaces 146 (2016) 700-706 (October)

Effect of mechanical denaturation on surface free energy of protein powders

Mohammad Amin Mohammad[a,b*], Ian M. Grimsey[a], Robert T. Forbes[a]
Ian S. Blagbrough[c], Barbara R Conway[d]

[a] School of Pharmacy, University of Bradford, Bradford, BD7 1DP, UK.
[b] Faculty of Pharmacy, University of Damascus, Damascus, Syria.
[c] Department of Pharmacy and Pharmacology, University of Bath, Bath BA2 7AY, UK.
[d] Department of Pharmacy, University of Huddersfield, Queensgate, Huddersfield, HD1 3DH, UK.

Dr. Ian S. Blagbrough: Phone: +44 (0) 1225 386795; Email: prsisb@bath.ac.uk

ABSTRACT

Globular proteins are important both as therapeutic agents and excipients. However, their fragile native conformations can be denatured during pharmaceutical processing, which leads to modification of the surface energy of their powders and hence their performance. Lyophilized powders of hen egg-white lysozyme and β-galactosidase from *Aspergillus oryzae* were used as models to study the effects of mechanical denaturation on the surface energies of basic and acidic protein powders, respectively. Their mechanical denaturation upon milling was confirmed by the absence of their thermal unfolding transition phases and by the changes in their secondary and tertiary structures. Inverse gas chromatography detected differences between both unprocessed protein powders and the changes induced by their mechanical denaturation. The surfaces of the acidic and basic protein powders were relatively basic, however the surface acidity of β-galactosidase was higher than that of lysozyme. Also, the surface of β-galactosidase powder had a higher dispersive energy compared to lysozyme. The mechanical denaturation decreased the dispersive energy and the basicity of the surfaces of both protein powders. The amino acid composition and molecular conformation of the proteins explained the surface energy data measured by inverse gas chromatography. The biological activity of mechanically denatured protein powders can either be reversible (lysozyme) or irreversible (β-galactosidase) upon hydration. Our surface data can be exploited to understand and predict the performance of protein powders within pharmaceutical dosage forms.

Keywords: Protein denaturation; β-Galactosidase; Lysozyme; Conformational change; Inverse gas chromatography; Surface free energy.

1. Introduction

In the pharmaceutical field, there is considerable interest in the use of globular proteins for their therapeutic effects. During pharmaceutical processes, protein powders are often subjected to mechanical stresses. For example, milling has been used to prepare protein particles suitable for pulmonary delivery and protein-loaded microparticles in industrial quantities [1,2]. The mechanical stresses applied during the milling can partially or completely denature the proteins and change their bulk properties [3]. In recent years, denatured globular proteins have found extensive applications as excipients in pharmaceutical formulations [4,5]. Denatured globular proteins have been used to prepare emulsion systems designed to enhance the absorption of insoluble drugs and to form nanoparticles for drug delivery and targeting [4]. Globular proteins have also been successfully used to formulate controlled drug delivery tablets, which delay drug release in gastric conditions by forming a gel-layer stabilized by intermolecular–beta sheets of denatured globular proteins [5].

Surface energies of powders are critical properties to be considered during formulation and development of dosage forms in the pharmaceutical industry. Surface energy has significant effects on pharmaceutical processes such as granulation, tableting, disintegration, dissolution, dispersibility, immiscibility, wettability, adhesion, flowability, packing etc. Resultant data from recent determination of surface energies have been used to reduce the time of formulation development and enhance the quality of the final product [6-8].

The effect of the protein denaturation on their surface chemistry has been determined using time-of-flight secondary ion mass spectrometry [9]. However, the effect of mechanical denaturation on the surface energies of globular proteins has not been reported and these effects must be understood to exploit the full potential of globular proteins in pharmaceutical industry both as

therapeutic agents and excipients. Inverse gas chromatography (IGC) is a useful verified tool for surface energy measurements [10]. IGC has been used to measure the surface free energy of lyophilized protein particles, detecting lot-to-lot variations in the amorphous microstructure of lyophilized protein formulations [11].

This paper aims to evaluate the effects of mechanical denaturation on the surface energies of globular protein powders using IGC. β-Galactosidase is a hydrolytic enzyme that has been widely investigated for potential applications in the food industry to improve sweetness, solubility, flavor, and digestibility of dairy products. Preparations of β-galactosidases have also been exploited for industrial, biotechnological, medical, and analytical applications [12]. Lysozyme is a naturally occurring enzyme found in bodily secretions such as tears, saliva, and milk and has been explored as a food preservative and pharmaceutical. The isoelectric points (pI) of β-galactosidase from *Aspergillus oryzae* and hen egg-white lysozyme are 4.6 and 11.3, and these proteins were used as models of acidic and basic globular proteins, respectively [13]. Lyophilized powders of these proteins were mechanically denatured by milling. Their surface energies before and after denaturation were compared in order to understand how the surfaces of the globular protein powders respond to the mechanical denaturation.

2. Materials and methods

2.1. Materials

Micrococcus lysodeikticus (Sigma-Aldrich), 2-nitrophenyl β-D-galacto pyranoside (Sigma-Aldrich), lyophilized powders of β-galactosidase from *A. oryzae* (Sigma-Aldrich) and hen egg-white lysozyme (Biozyme Laboratories, UK) were purchased as indicated. The purchased β-galactosidase

and lysozyme powders were considered to be unprocessed samples and named UNG and UNL, respectively.

2.2. Preparation of mechanically denatured protein powders

Mechanically denatured powders of β-galactosidase and lysozyme were prepared by manually milling. The milling was achieved by rotating a marble pestle over the powder within a marble mortar at ~45 cycles per minute (cpm). Milling times of 60 min were enough to completely denature the protein powders, and this was confirmed by differential scanning calorimetry (DSC) [3]. The mechanically denatured powders of β-galactosidase and lysozyme were named DeG and DeL, respectively. Three batches (2 g each batch) of the mechanically denatured powders were prepared for each protein.

2.3. Microscopy

A Zeiss Axioplan2 polarizing microscope (Carl Zeiss Vision GmbH; Hallbergmoos, Germany) was used to visualize the samples. The accompanying software (Axio Vision 4.2) was then used to determine the projected area diameters of the powders.

2.4. Differential scanning calorimetry (DSC)

Differential scanning calorimetry (DSC) thermograms were obtained using a Perkin-Elmer Series 7 DSC (Perkin-Elmer Ltd., Beaconsfield, UK). Samples (4-7 mg) were sealed in aluminium pans. The escape of water was facilitated by making a pinhole in the lid prior to sealing. The samples were equilibrated at 25 °C and heated to 250 °C at a scan heating rate of 10 °C/min under a flow of anhydrous nitrogen (20 ml/min). Each sample was analysed in triplicate. The temperature axis and

cell constant of the DSC cell were calibrated with indium (10 mg, 99.999 % pure, melting point 156.60 °C, and heat of fusion 28.40 J/g).

2.5. FT-Raman spectroscopy

FT-Raman spectra of samples were recorded with a Bruker IFS66 optics system using a Bruker FRA 106 Raman module. The excitation source was an Nd: YAG laser operating at 1064 nm and a laser power of 50 mW was used. The FT-Raman module was equipped with a liquid nitrogen cooled germanium diode detector with an extended spectrum band width covering the wave number range 1800-450 cm^{-1}. Samples were placed in stainless steel sample cups and scanned 200 times with the resolution set at 8 cm^{-1}. The observed band wave numbers were calibrated against the internal laser frequency and are correct to better than ±1 cm^{-1}. The spectra were corrected for instrument response. The experiments were run at a controlled room temperature of 20±1°C.

2.6. Enzymatic assay

The enzymatic activity of lysozyme samples was measured to determine the ability of lysozyme to catalyze the hydrolysis of β-1,4-glycosidic linkages of cell-wall mucopolysaccharides [14]. Lysozyme solution (30 µl, 0.05 % in phosphate buffer, pH = 5.2; 10 mM) was added to *Micrococcus lysodeikticus* suspension (2.97 ml, 0.025 % in phosphate buffer, pH = 6.24; 66 mM). The decrease in the absorbance at 450 nm was monitored by using a UV-Vis spectrophotometer (PU 8700, Philips, UK). The activity was determined by measuring the decrease in the substrate bacterial suspension concentration with time. Hence the slope of the reduction in light absorbance at 450 nm against the time of 3 min, starting when the protein solutions were mixed with the substrate bacterial suspension, was considered to be the indicator of the lytic activity of lysozyme [15].

The enzymatic activity of β-galactosidase samples was determined using a method relying on the ability of β-galactosidase to hydrolyse the chromogenic substrate *o*-nitrophenyl β-D-galacto pyranoside (ONPG) to *o*-nitrophenol [16]. The results were achieved by adding 20 μl of protein solution (0.05 w/v% in deionised water) to 4 ml of the substrate solution (0.665 mg/ml) in a phosphate buffer (100 mM and pH = 7). The mixture then was incubated for 10 min in a water bath at 30±1 °C. The absorbance at λ = 420 nm was measured to indicate the activity.

The concentrations of the protein solutions had been determined prior to the activity tests using the following equation:

$$[Protein] = Abs_{280\,nm}/E_{280\,nm} \qquad (1)$$

where $[Protein]$ is the concentration of protein in the tested solution w/v%, $Abs_{280\,nm}$ is the absorbance of the tested protein solution at 280 nm, and $E_{280\,nm}$ is the absorbance of protein standard solution with concentration 0.05 w/v%. The concentrations of the solutions were diluted to be about 0.05 % w/v so as to give an absorbance value of less than 0.8. The activities of all samples were measured relative to that of a corresponding fresh sample, which was considered as the standard solution.

2.7. Inverse gas chromatography

IGC experiments were performed using an inverse gas chromatography (IGC 2000, Surface Measurement Systems Ltd., UK). A sample (~500 mg) was packed into a pre-silanised glass column (300 mm × 3 mm i.d.). Three columns of each sample were analysed at 30 °C (the lowest temperature at which the IGC experiments can be performed to avoid thermal stress) and zero relative humidity,

148 using anhydrous helium gas as the carrier. A series of n-alkanes (n-hexane to n-nonane) in addition
149 to chloroform, as a monopolar electron acceptor probe (l_+), and ethyl acetate, as a monopolar donor
150 acceptor probe (l_-), were injected through the columns at the infinite dilution region. Their retention
151 times followed from detection using a flame ionization detector (FID).
152
153 *2.7.1. Surface energy calculations*
154 Our published methods were used to calculate the surface energies and verify their accuracy
155 [17-19]. These methods describe the surface properties using the dispersive retention factor ($K^a_{CH_2}$),
156 the electron acceptor retention factor (K^a_{l+}), and the electron donor retention factor (K^a_{l-}), which are
157 calculated using the retention times of probes:

158 $$\ln (t_r - t_0) = (\ln K^a_{CH_2})\, n + C \qquad (2)$$

159 where n is the carbon number of the homologous n-alkanes, t_r and t_0 are the retention times of the n-
160 alkanes and a non-adsorbing marker, respectively, $K^a_{CH_2}$ is the dispersive retention factor of the
161 analysed powder and C is a constant. The linear regression statistics of equation 2 generate the value
162 of t_0 which gives its best linear fit. The slope of the equation 2 gives the value of $K^a_{CH_2}$.

163 $$K^a_{l+} = t_{nl+}/t_{nl+,ref} \qquad (3)$$

164 $$K^a_{l-} = t_{nl-}/t_{nl-,ref} \qquad (4)$$

165 where t_{nl+} and $t_{nl+,ref}$ are the retention time of l_+ and its theoretical n-alkane reference, respectively,
166 t_{nl-} and $t_{nl-,ref}$ are the retention time of l_- and its theoretical n-alkane reference, respectively.

167 $$\ln t_{nl+,ref} = \ln t_{nCi} + \left(\frac{\alpha_{l+}\left(\gamma^d_{l+}\right)^{0.5} - \alpha_{Ci}\left(\gamma^d_{Ci}\right)^{0.5}}{\alpha_{CH_2}\left(\gamma_{CH_2}\right)^{0.5}} \right) \ln K^a_{CH_2} \qquad (5)$$

168 $$\ln t_{nl-,ref} = \ln t_{nCi} + \left(\frac{\alpha_{l-}\left(\gamma^d_{l-}\right)^{0.5} - \alpha_{Ci}\left(\gamma^d_{Ci}\right)^{0.5}}{\alpha_{CH_2}\left(\gamma_{CH_2}\right)^{0.5}} \right) \ln K^a_{CH_2} \qquad (6)$$

where α_{CH_2} and γ_{CH_2}, α_{Ci} and γ_{Ci}^{d}, α_{l+} and γ_{l+}^{d}, and α_{l-} and γ_{l-}^{d} are the cross–sectional area and the dispersive free energy of a methylene group, an n-alkane, l_+ and l_-, respectively. t_{nCi} is the retention time of the n-alkane.

The retention factors are then used to calculate the surface dispersive (γ_s^d), electron donor (γ_s^-) and electron acceptor (γ_s^+) components of the powders:

$$\gamma_s^d = \frac{0.477\,(T \ln K_{CH_2}^a)^2}{(\alpha_{CH_2})^2\,\gamma_{CH_2}} \text{ mJ.m}^{-2} \quad (7)$$

$$\gamma_s^- = \frac{0.477\,(T \ln K_{l+}^a)^2}{(\alpha_{l+})^2\,\gamma_{l+}^+} \text{ mJ.m}^{-2} \quad (8)$$

$$\gamma_s^+ = \frac{0.477\,(T \ln K_{l-}^a)^2}{(\alpha_{l-})^2\,\gamma_{l-}^-} \text{ mJ.m}^{-2} \quad (9)$$

where γ_{l+}^+ is the electron acceptor component of l_+ and γ_{l-}^- is the electron donor component of l_-. The units of α are Å^2 and of γ are mJ.m^{-2} in all equations.

The parameters of CH_2 are calculated from the following equation:

$$(\alpha_{CH_2})^2\,\gamma_{CH_2} = -1.869T + 1867.194 \text{ Å}^4\text{.mJ.m}^{-2} \quad (10)$$

The parameters of polar probes are still under debate and different values have been reported [20-25]. In this paper, we used the values which were recently used for ethyl acetate (γ_{l-}^-= 19.20 mJ/m^2, γ_{l-}^d= 19.60 mJ/m^2, α_{l-}= 48.0 Å^2) and for chloroform (γ_{l+}^+= 3.80 mJ/m^2, γ_{l+}^d= 25.90 mJ/m^2, α_{l+}= 44.0 Å^2) [17,22]. However, using any other different reported numbers will not change the findings of the comparison.

The percentage coefficient of variation of ln $K_{CH_2}^a$ ($\%CV_{\ln K_{CH_2}^a}$) is the indicator of the accuracy of the surface energy measurements. The error of the slope of the equation 2 ($SD_{\ln K_{CH_2}^a}$) is used to calculate $\%CV_{\ln K_{CH_2}^a}$:

$$\%CV_{\ln K^a_{CH_2}} = \left(SD_{\ln K^a_{CH_2}} / \ln K^a_{CH_2}\right) \times 100 \quad (11)$$

$\%CV_{\ln K^a_{CH_2}}$ should be less than 0.7% to accept the accuracy of the measurement. $\%CV_{\ln K^a_{CH_2}}$ is then used to calculate the uncertainty range of γ_s^d:

$$\text{Uncertainty Range of } \gamma_s^d = \left[\left(\frac{100\times\gamma_s^d}{100+7.5\%CV_{\ln K^a_{CH_2}}}\right) to \left(\frac{100\times\gamma_s^d}{100-7.5\%CV_{\ln K^a_{CH_2}}}\right)\right] \quad (12)$$

3. Results and discussion

3.1. Microscopy

The photomicrographs of UNL, UNG, DeL, and DeG powders show that they had project-area diameters of ~4 μm (Fig. S1), ~2.5 μm (Fig. S2), ~1.5 μm (Fig. S3), and ~1.5 μm (Fig. S4), respectively. The particle sizes of the original powders were below 5 μm. Therefore, the attrition mechanism was dominant during milling, and so the same original faces did not change [3].

3.2. Differential scanning calorimetry (DSC)

For both proteins, DSC thermograms exhibited broad peaks ranging from ~30 to ~140 °C (Figure 1). These peaks are due to water removal, and their areas depend on water residues in the powders [3]. The enthalpy of the water evaporation peak was 118±11, 124±6, 114±9 and 130±8 J/g for UNL, UNG, DeL, and DeG, respectively, and did not significantly change after milling (t-test: $P < 0.05$). The protein powders exchange water with the surrounding air depending on conditions of temperature, relative humidity and exposure time. Therefore, the conditions used during milling did not change the water content of the powders. Also, Fig. 1 shows that the unprocessed proteins unfolded and a peak was detected at their apparent denaturation temperatures, which varied according

to the protein. DSC thermograms of UNL displayed one denaturation peak at ~201 °C, but UNG displayed two denaturation peaks at ~176 °C and ~212 °C.

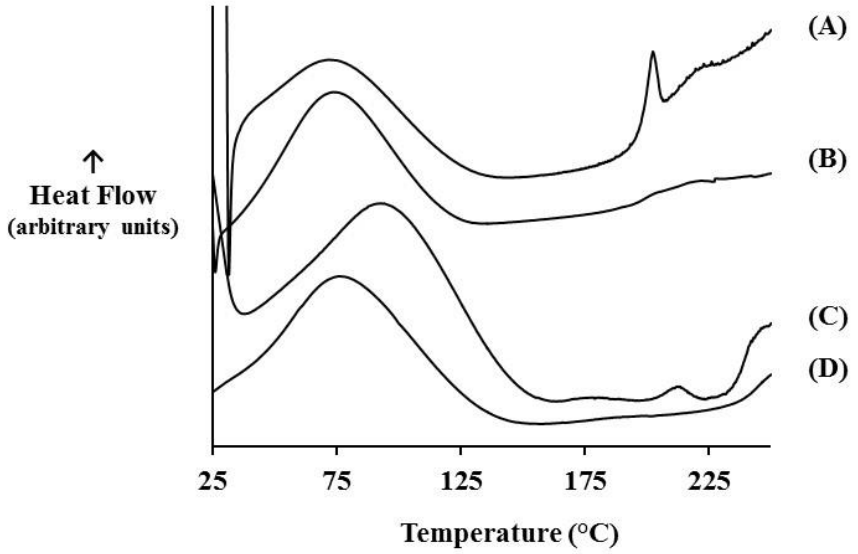

Fig. 1. Example DSC thermograms of protein powders (A) unprocessed lysozyme, (B) mechanically denatured lysozyme, (C) unprocessed β-galactosidase, (D) mechanically denatured β-galactosidase. Conditions: samples heated from 25 to 250 °C; heating rate: 10 °C/min.

The difference in the thermal denaturation pattern can be due to the difference in the thermal unfolding mechanisms of the proteins. While lysozyme folds in a highly cooperative manner and so exhibits an all-or-none thermal unfolding transition, β-galactosidase goes through a non-two state thermal unfolding transition resulting in two peaks [26,27]. The unfolding transition peaks were completely lost after mechanical denaturation. Hence there was no peak at ~201 ºC for the milled lysozyme samples and neither were there peaks at ~176 °C and ~212 °C for the milled β-galactosidase. The complete disappearance of the unfolding transition peak from the DSC thermogram indicates the total transition of the protein from its folded state to its unfolded state [3].

222 *3.3. FT-Raman study*

223 Raman spectroscopy was used to compare the molecular conformation of protein powders
224 before and after mechanical denaturation. The band at ~1450 cm^{-1} indicates the CH bending
225 vibrations of aliphatic side chains, and its intensity and position are unaffected by changes induced
226 in protein structure after dehydration or applying different stresses [28]. Therefore, it was used as an
227 internal intensity standard to normalize Raman spectra before comparison (Figures 2A and 3A). The
228 vibration modes of amide I (C=O stretch) from 1580 to 1720 cm^{-1} (Figures 2B and 3B) and amide III
229 (N-H in-plane bend + C-N stretch) from 1250–1330 cm^{-1} (Figures 2C and 3C) demonstrated the
230 secondary structure of β-galactosidase and lysozyme, respectively. The spectra of the denatured
231 samples show that the modes of the amide I upshifted and broadened for both proteins, and the mode
232 of the amide III intensified and downshifted, especially for lysozyme, but there was no change in the
233 mode of amide III for β-galactosidase. These changes indicated the transformation of α-helix content
234 to β-sheets or a disordered structure which enhances the tendency of proteins to aggregate [3,29].
235 While β-galactosidase is a beta-type protein containing mainly β-sheet structure and only 5% α-helix
236 [30], the secondary structure of lysozyme consists of 30% α-helix [31]. This explains why no changes
237 in the amide III of β-galactosidase were observed.

238 The aggregation of denatured proteins combined with changes in the vibration modes of the
239 aromatic residues at ~1550 cm^{-1} in β-galactosidase (Figure 2D), 1320-1380 cm^{-1} in lysozyme (Figure
240 3D) and 800-900 cm^{-1} in both proteins (Figures 2E and 3E). These changes in the vibration modes of
241 the aromatic residues result from the changes in their micro-environment after denaturation because
242 of their roles in the denaturation processes [29,32]. The aggregates of denatured protein molecules
243 are formed via π-stacking interactions of the aromatic residues [33].

(A)

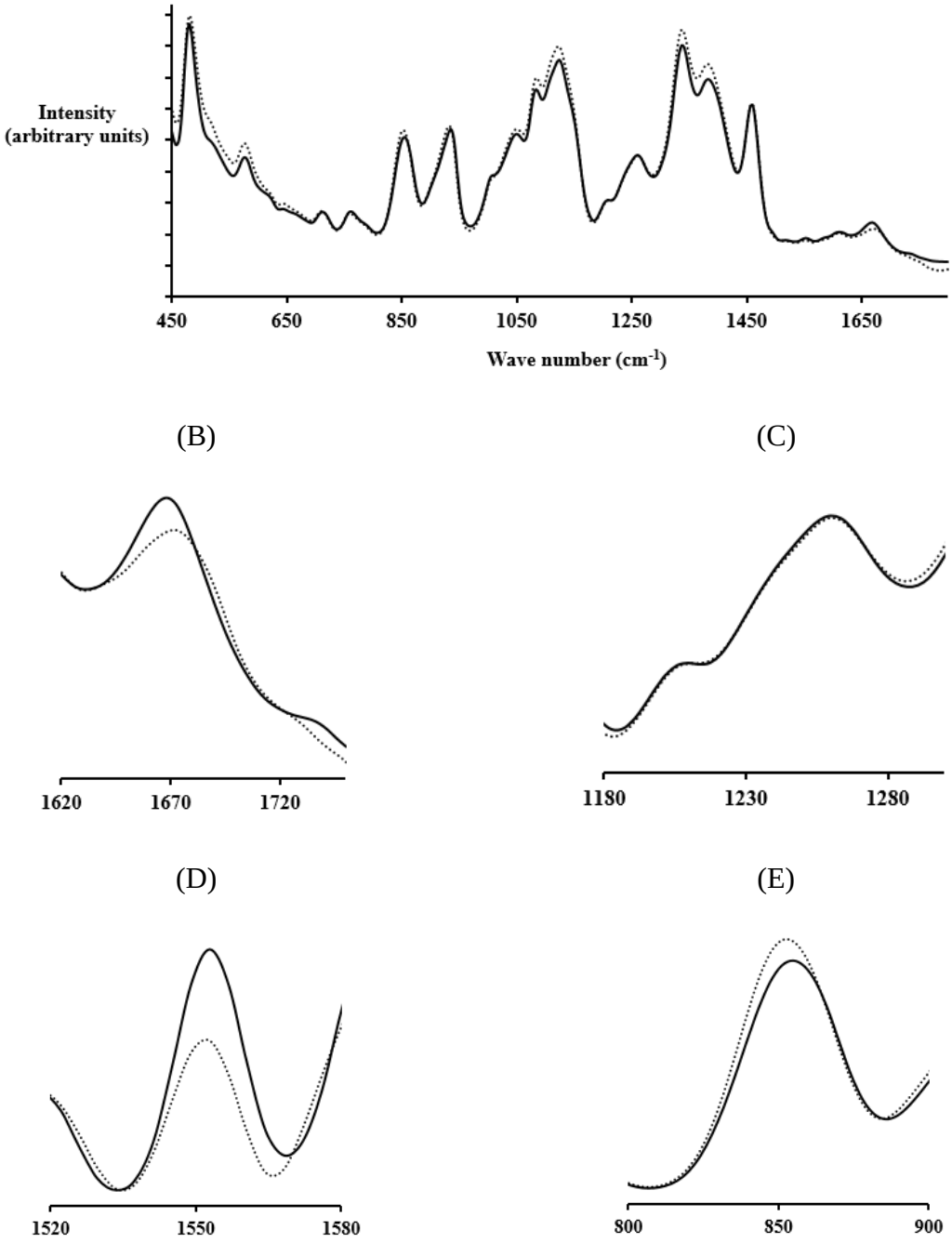

Fig. 2. FT-Raman spectra of β-galactosidase powders, the unprocessed powders (solid lines) and the mechanically denatured powders (dotted lines). Vibration modes of secondary structure are (B) amide I and (C) amide III. Vibration modes of tertiary structure are (D) for Trp and (E) for Trp and Tyr. The spectra were normalized using the methylene deformation mode at ~1450 cm^{-1} as an internal intensity standard.

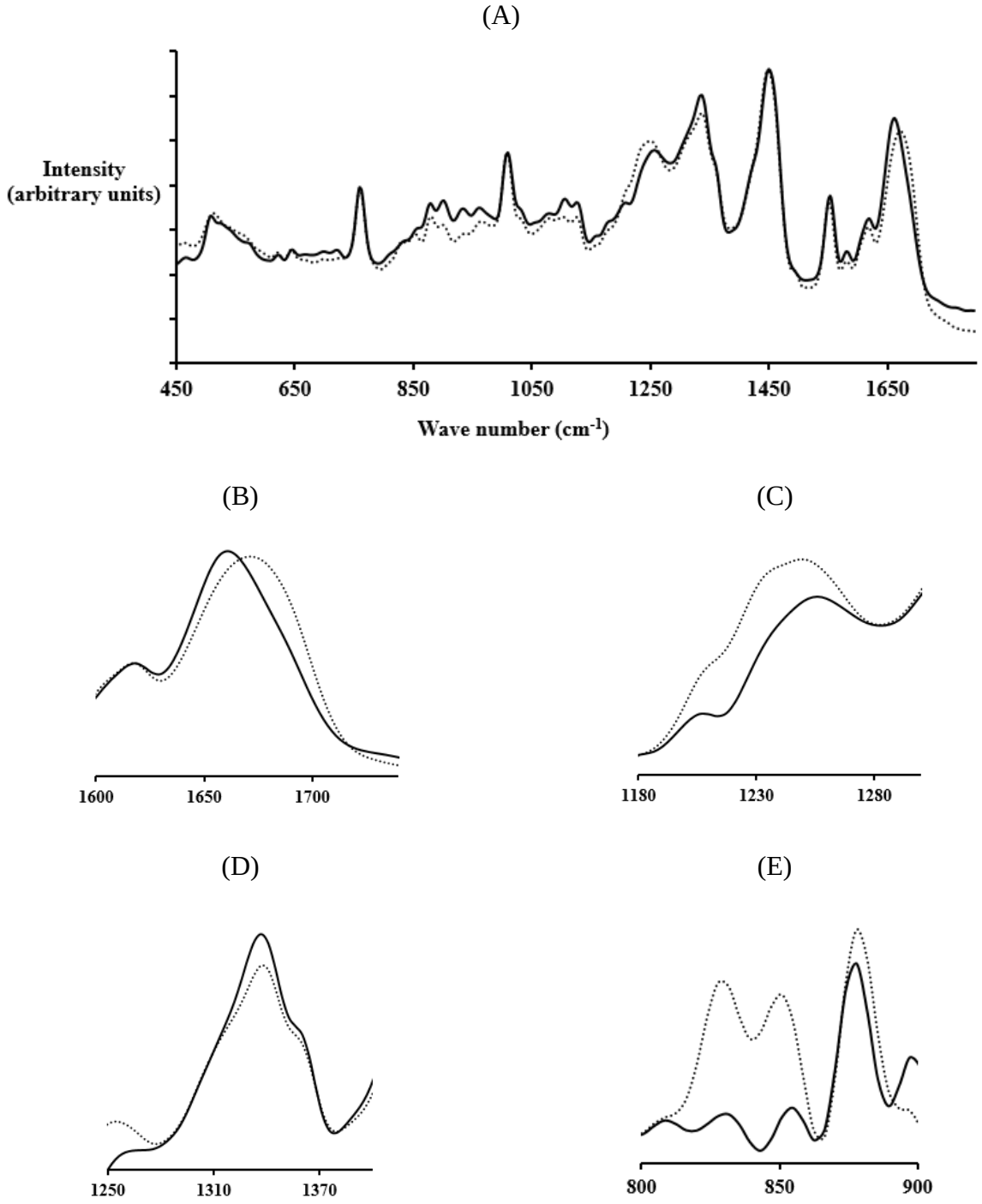

Fig. 3. FT-Raman spectra of lysozyme powders, the unprocessed powders (solid lines) and the mechanically denatured powders (dotted lines). Vibration modes of secondary structure are (B) amide I and (C) amide III. Vibration modes of tertiary structure are (D) for Trp and (E) for Trp and Tyr. The spectra were normalized using the methylene deformation mode at ~1450 cm^{-1} as an internal intensity standard.

3.4. Enzymatic assay

Therapeutic proteins may rapidly denature and lose their enzymatic activity. The structure changes detected using FT-Raman and the absence of Tm detected by DSC have been used to monitor the denaturation of proteins, and the results of Raman and DSC are linked to the results of enzymatic activity [34]. Our DSC and Raman results confirmed the denaturation of both proteins studied. The enzymatic assay showed that the mechanically denatured β-galactosidase samples (DeG) demonstrated no enzymatic activity (Figure 4). However, the mechanically denatured lysozyme samples (DeL) maintained full enzymatic activity when compared to an unprocessed sample (t-test: $P < 0.05$) (Figure 4). This is due to the ability of denatured lysozyme to refold upon dissolution in aqueous media and thus the biological activity of lysozyme is fully recovered following dissolution [3.35].

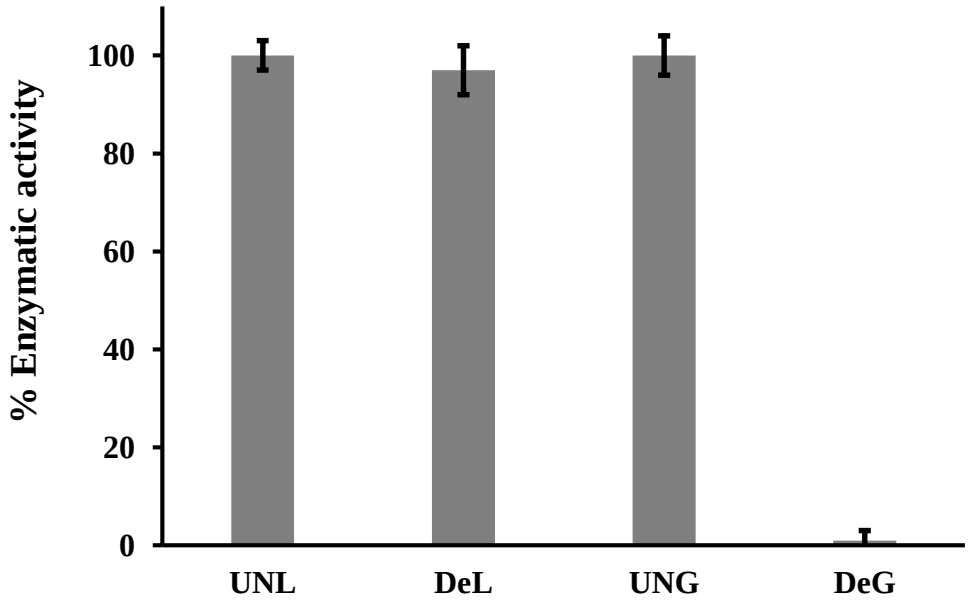

Fig. 4. Enzymatic activity of the unprocessed powders and the mechanically denatured powders of lysozyme and β-galactosidase.

3.5. Surface free energy

The IGC results (Table 1) confirm the acceptable accuracy of the IGC experiments considered in this work with $\%CV_{\ln K^a_{CH_2}}$ values of less than 0.7% [18]. IGC data for the unprocessed powders demonstrated the differences in the surface free energy between β-galactosidase (an acidic protein) and lysozyme (a basic protein). UNG had higher γ_s^d compared to UNL because the uncertainty ranges of γ_s^d of UNG and UNL did not overlap for the three columns [18]. The surface acidity (γ_s^+) and the surface basicity (γ_s^-) of UNG were significantly different from their counterparts of UNL (t-test: $P < 0.05$). The average of γ_s^+ was 16.2±0.2 and 12.4±0.1 mJ.m^{-2} and the average of γ_s^- was 5.5±0.2 and 10.5±0.6 mJ.m^{-2} for UNG and UNL, respectively. This proves that UNG, chosen as a model for acidic proteins, has higher surface acidity and lower surface basicity compared to selected basic protein, UNL.

Table 1. The surface energies (γ_s^d, γ_s^+ and γ_s^-) and retention factors ($K^a_{CH_2}$, K^a_{l+} and K^a_{l-}) of the lyophilized lysozyme powder (UNL), the lyophilized β-galactosidase powder (UNG), the mechanically denatured lyophilized lysozyme powder (DeL) and the mechanically denatured lyophilized β-galactosidase powder (DeG).

Material	Column	$K^a_{CH_2}$	K^a_{l+}	K^a_{l-}	$\%CV_{\ln K^a_{CH_2}}$	γ_s^d mJ.m^{-2}	Uncertainty Range of γ_s^d mJ.m^{-2}	γ_s^+ mJ.m^{-2}	γ_s^- mJ.m^{-2}
UNL	1	3.099	3.725	34.572	0.144	43.1	41.9-44.4	12.4	10.3
UNL	2	3.095	3.677	34.668	0.094	43.0	42.2-43.9	12.5	10.1
UNL	3	3.089	3.944	33.704	0.077	42.9	42.2-43.6	12.3	11.2
DeL	1	2.937	2.781	33.948	0.127	39.1	38.1-40.2	12.3	6.2
DeL	2	2.965	2.742	31.928	0.147	39.8	38.7-41.0	11.9	6.1
DeL	3	2.944	2.801	31.826	0.117	39.3	38.4-40.3	11.9	6.3
UNG	1	3.235	2.542	55.641	0.141	46.5	45.1-47.8	16.0	5.2
UNG	2	3.222	2.640	58.508	0.076	46.1	45.4-46.9	16.4	5.6
UNG	3	3.228	2.625	56.028	0.158	46.3	44.8-47.9	16.1	5.6
DeG	1	2.926	1.980	43.387	0.205	38.9	37.3-40.6	14.1	2.8
DeG	2	2.958	1.829	41.065	0.160	39.7	38.4-41.0	13.7	2.2
DeG	3	2.948	1.841	39.710	0.221	39.4	37.7-41.3	13.4	2.2

The isoelectric point (pI) of a protein indicates its relative acidity or basicity, the higher the pI, the higher the basicity of the molecule [36]. The isoelectric points (pI) of the β-galactosidase and lysozyme used are 4.6 and 11.3, respectively [13]. The molecule of β-galactosidase contains ~11 w/w% basic amino acids (histidine, lysine, and arginine) and ~22 w/w% acidic (aspartic acid and glutamic acid) residues [37], i.e., approximately double the number of acidic groups compared to basic. Conversely the lysozyme contains ~18 w/w% and ~7 w/w% basic (histidine, lysine, and arginine) and acidic (aspartic acid and glutamic acid) residues, respectively [38]. Detailed information regarding the structures of β-galactosidase and lysozyme can be found in [37,38]. However, this is not the only determinant of energy as the surfaces of both the acidic (UNG) and basic (UNL) protein powders were relatively basic (the values of $\gamma_s^+ > \gamma_s^-$). Therefore to explain our results further, the interaction of protein molecules with surfaces and interfaces, during preparation using lyophilization technique, must be considered.

As protein molecules are surface active containing both polar and nonpolar groups, they tend to adsorb to interfaces via hydrophobic interactions (London), coulombs (electrostatic) and/or hydrogen bonding, and they reorient their surfaces to the parts which give the optimum attractive force and the most stable state (minimum energy) with a substrate or an interface [39]. Upon lyophilization, protein molecules adsorb to the formed ice via hydrophobic residues but not via hydrophilic residues, and this gives support to the hypothesis that the interaction of proteins with ice involves appreciable hydrophobic interactions [40]. The hydrophobic regions in protein molecules interact spontaneously with the ice faces by an entropy driving force [41]. The rich electron rings of aromatic residues orient so that the ring structures lie flat with the interface in order to maximize the interaction at interfaces and lower the Gibbs free energy of the system [42]. Therefore, lyophilized protein particles expose the rich electron rings of the aromatic residues on their surfaces. Aromatic

groups, via their π electrons, which are considered nucleophilic, can form hydrogen bonds with chemical groups (acidic polar probes) being the hydrogen donors [43]. Therefore, exposing these rings to surfaces relatively increases their basicity compared to their acidity irrespective of the acidic or basic nature of the proteins themselves. Also the ring structures can participate in raising the dispersive surface energy via London interactions due to their high polarizability [43]. The aromatic residues (tryptophan, tyrosine, and phenylalanine) make up 16%w/w of the β-galactosidase molecules and 14%w/w of the lysozyme molecules [37,38]. This explains the higher values of γ_s^d of β-galactosidase compared to lysozyme, prior to mechanical denaturation.

UNG was more acidic than UNL. The size and the shape of the molecule can also influence orientation. UNG is larger than UNL, with a globular shape and when some of the chemical groups are preferably exposed to a surface (energetically or entropically), this will expose not only those specific groups but also other closely associated groups which will vary in nature from one protein to another.. Thus, the surfaces of the acidic protein (β-galactosidase) were more acidic compared to the basic protein (lysozyme).

Table 1 shows that mechanical denaturation decreased the dispersive free energy and the basicity of the surfaces of protein powders, irrespective of the nature of the protein (acidic or basic). Usually milling induces an increase in the dispersive energy due to the generation of surface amorphous regions or/and creation of higher energy crystal faces because of particle fracture/breakage, thus the surface acidity and basicity change according to the formation of new faces and regions [44,45]. However, in our case, due to lyophilization, the protein powders are amorphous with particle sizes below 5 μm. Therefore, there would be no further size reduction by fracture mechanisms because of brittle ductile transition [3]. Therefore, the denatured protein powders were produced by milling where the attrition mechanism was dominant and so the same original faces did not change. During

337 milling, the extensive mechanical energy completely denatured the protein molecules as confirmed
338 by DSC and Raman results. This denaturation led to aggregation of the protein molecules via non-
339 covalent interactions through π-stacking interactions [33]. This caused a loss of the aromatic groups,
340 which are rich in π electrons, from the surfaces. Therefore, a decrease in the Van der Waals
341 interactions, a major contributor to dispersive energy and nucleophilicity (basicity) occurred, and so
342 γ_s^d and γ_s^- decreased after denaturation for both proteins. Also, this loss of aromatic residues from the
343 surface of the denatured powders renders γ_s^d similar for both proteins. This is further evidence that
344 the exposed aromatic residues raise the γ_s^d as outlined previously. The Raman spectroscopic results
345 confirmed that the aromatic residues were involved in the denaturation processes, therefore,
346 supporting the findings and our interpretation of the IGC studies.
347
348 **4. Conclusions**
349 The surface energies of the lyophilized protein powders differed according to their amino acid
350 compositions. The absence of the thermal unfolding transition phase for the proteins (lysozyme and
351 β-galactosidase) and the changes in the conformation of the back-bone and side chains confirmed
352 that the mechanical milling process caused denaturation of the protein powders, and this denaturation
353 could potentially be reversible in solution. The acidic protein powder (β-galactosidase) had higher
354 surface acidity (γ_s^+) and lower surface basicity (γ_s^-) compared to the basic protein powder (lysozyme).
355 However, both protein powders had relatively basic surfaces due to the rich electron rings of the
356 aromatic residues which are nucleophilic. During mechanical denaturation, these rings tend to
357 associate through π-stacking interactions and are thus concealed from the surface. Their removal

reduced γ_s^- and γ_s^d of the surfaces of both protein powders, and thereby yielded similar γ_s^d for the surfaces of both proteins.

Acknowledgements

MAM gratefully acknowledges CARA (Stephen Wordsworth and Ryan Mundy) the Universities of Bath and Bradford for providing academic fellowships.

Appendix A: Supplementary data

Supplementary data associated with this article can be found, in the online version, at http://dx.doi.org/10.1016/j.colsurfb.2016.07.

References

[1] H. Hoyer, W. Schlocker, K. Krum, A. Bernkop-Schnürch, Eur. J. Pharm. Biopharm. 69 (2008) 476.
[2] W. Schlocker, S. Gschliesser, A. Bernkop-Schnürch, Eur. J. Pharm. Biopharm. 62 (2006) 260.
[3] M.A. Mohammad, I.M. Grimsey, R.T. Forbes, J. Pharm. Biomed. Anal. 114 (2015) 176.
[4] W. He, K. Yang, L. Fan, Y. Lv, Z. Jin, S. Zhu, C. Qin, Y. Wang, L. Yin, Int. J. Pharm. 495 (2015) 9.
[5] R. Caillard, M. Subirade, Int. J. Pharm. 437 (2012) 130.
[6] V. Karde, C. Ghoroi, Int. J. Pharm. 475 (2014) 351.
[7] X. Han, L. Jallo, D. To, C. Ghoroi, R. Davé, J. Pharm. Sci. 102 (2013) 2282.
[8] D. Cline, R. Dalby, Pharm. Res. 19 (2002) 1274.
[9] M.S. Killian, H.M. Krebs, P. Schmuki, Langmuir 27 (2011) 7510.
[10] O. Planinsek, A. Trojak, S. Srcic, Int. J. Pharm. 221 (2001) 211.
[11] Y. Hirakura, H. Yamaguchi, M. Mizuno, H. Miyanishi, S. Ueda, S. Kitamura, Int. J. Pharm. 340 (2007) 34.
[12] Q. Husain, Crit. Rev. Biotechnol. 30 (2010) 41.
[13] M. Ospinal-Jiménez, D.C. Pozzo, Langmuir 28 (2012) 17749.
[14] R.R. Haj-Ahmad, A.A. Elkordy, C.S. Chaw, A. Moore, Eur. J. Pharm. Sci. 49 (2013) 519.
[15] S. Chakraborti, T. Chatterjee, P. Joshi, A. Poddar, B. Bhattacharyya, S.P. Singh, V. Gupta, P. Chakrabarti, Langmuir 26 (2010) 3506.
[16] R.E. Hamlin, T.L. Dayton, L.E. Johnson, M.S. Johal, Langmuir 23 (2007) 4432.
[17] M.A. Mohammad, J. Chromatogr. A 1318 (2013) 270.

[18] M.A. Mohammad, J. Chromatogr. A 1399 (2015) 88.
[19] M.A. Mohammad, J. Chromatogr. A 1408 (2015) 267.
[20] B. Shi, D. Qi, J. Chromatogr. A 1231 (2012) 73.
[21] C. Della Volpe, D. Maniglio, M. Brugnara, S. Siboni, M. Morra, J. Colloid Interface Sci. 271 (2004) 434.
[22] S.C. Das, I. Larson, D.A. Morton, P.J. Stewart, Langmuir 27 (2011) 521.
[23] C.D. Volpe, S. Siboni, J. Colloid Interface Sci. 195 (1997) 121.
[24] J. Schultz, L. Lavielle, C. Martin, J. Adhesion 23 (1987) 45.
[25] C.J. Van Oss, R.J. Good, M.K. Chaudhury, Langmuir 4 (1988) 884.
[26] B. Maroufi, B. Ranjbar, K. Khajeh, H. Naderi-Manesh, H. Yaghoubi, Biochim. Biophys. Acta 1784 (2008) 1043.
[27] J.M. Sánchez, V. Nolan, M.A. Perillo, Colloids Surf. B Biointerfaces 108 (2013) 1.
[28] T.J. Yu, J.L. Lippert, W.L. Peticolas, Biopolymers 12 (1973) 2161.
[29] E.N. Lewis, W. Qi, L.H. Kidder, S. Amin, S.M. Kenyon, S. Blake, Molecules 19 (2014) 20888.
[30] S.R. Tello-Solís, J. Jiménez-Guzmán, C. Sarabia-Leos, L. Gómez-Ruíz, A.E. Cruz-Guerrero, G.M. Rodríguez-Serrano, M. García-Garibay, J. Agric. Food Chem. 53 (2005) 10200.
[31] P.J. Artymiuk, C.C.F. Blake, D.W. Rice, K.S. Wilson, Acta Crystallogr. B: Struct. Crystallogr. Cryst. Chem. B38 (1982) 778.
[32] C. Zhou, W. Qi, E.N. Lewis, J.F. Carpenter, Anal. Biochem. 472 (2015) 7.
[33] S. Jang, J. Jang, W. Choe, S. Lee, ACS Appl. Mater. Interfaces 7 (2015) 1250.
[34] A. Torreggiani, M. Di Foggia, I. Manco, A. De Maio, S.A. Markarian, S. Bonora, J. Mol. Struct. 891 (2008) 115.
[35] A. Torreggiani, M. Tamba, I. Manco, M.R. Faraone-Mennella, C. Ferreri, C. Chatgilialoglu, J. Mol. Struct. 744 (2005) 767.
[36] C. Sun, J.C. Berg, Adv. Colloid Interface Sci. 105 (2003) 151.
[37] Y. Tanaka, A. Kagamiishi, A. Kiuchi, T. Horiuchi, J. Biochem. 77 (1975) 241.
[38] M.C. Vaney, S. Maignan, M. Riès-Kautt, A. Ducriux, Acta Crystallogr. D. Biol. Crystallogr. 52 (1996) 505.
[39] C. Chaiyasut, Y. Takatsu, S. Kitagawa, T. Tsuda, Electrophoresis 22 (2001) 1267.
[40] J. Baardsnes, P.L. Davies, Biochim Biophys Acta. 160 (2002) 49.
[41] S. Pezennec, F. Gauthier, C. Alonso, F. Graner, T. Croguennec, G. Brulé, A. Renault, Food Hydrocolloids 14 (2000) 463.
[42] M. Jurkiewicz-Herbich, A. Muszalska, R. Słojkowska, Colloids Surfaces A: Physicochem. Eng. Aspects 131 (1998) 315.
[43] G.I. Makhatadze, P.L. Privalov, Biophys. Chem. 50 (1994) 285.
[44] U.V. Shah, Z. Wang, D. Olusanmi, A.S. Narang, M.A. Hussain, M.J. Tobyn, J.Y. Heng, Int. J. Pharm. 495 (2015) 234.
[45] X. Han, L. Jallo, D. To, C. Ghoroi, R. Davé, J. Pharm. Sci. 102 (2013) 2282.